Origin of Coupling to Antisymmetric Cladding Modes in Arc-Induced Long-Period Fiber Gratings

O. V. Ivanov[*a], P. Caldas[a,b], and G. Rego[a,b]

[a]INESC Porto, Unidade de Optoelectrónica e Sistemas Electrónicos,
Rua do Campo Alegre 687, 4169-007 Porto, Portugal
[b]Escola Superior de Tecnologia e Gestão, Instituto Politécnico de Viana de Castelo,
Av. do Atlântico, Apartado 574, 4901-908 Viana do Castelo, Portugal

ABSTRACT

We study the origin of antisymmetric perturbation of the fiber in arc-induced long-period gratings that couple the core mode into the antisymmetric cladding modes. We demonstrate that this perturbation is caused by a temperature gradient in the fiber, which is induced, in turn, by a temperature gradient in the arc discharge.

Keywords: long-period fiber grating, electric arc discharge, microbend grating

1. INTRODUCTION

Long-period gratings (LPFGs) fabricated by the electric arc technique demonstrate some specific properties that make them attractive for applications in sensing and optical communications [1–3]. In particular, they have high temperature stability, exhibit good resistance to gamma radiation, and enable flexible tuning of their sensitivity to changes of physical parameters such as temperature and strain. The arc-induced LPFGs have been studied for quite a long-time; however, the mechanism of grating formation is still not well understood and there is a problem of reproducibility. As we have demonstrated recently, cladding modes of different symmetries are excited by LPFGs inscribed in different fibers by the same technique [4]. Therefore, different mechanisms are involved in the formation of arc-induced gratings. Among those mechanisms may be the modulation of core diameter due to fiber tapering under the arc discharge, strain induction or relaxation, microbending, and microdeformation.

LPFGs arc-induced in the SMF-28 fiber couple the core mode to the LP_{1i} cladding modes, being the corresponding perturbation antisymmetric. The origin of this asymmetry of the perturbation is unknown. In this paper, we investigate the process of grating inscription in more detail to find the asymmetric factor. In particular, we measure the temperature gradient in the arc and the resulting temperature gradient in the fiber. We discuss the contribution of the later gradient to the formation of LPFGs in the SMF-28 fiber. One of the consequences of the temperature gradient is the periodical microdeformation that consists in a shift of the fiber core under arc discharges. We analyze if such microdeformation can be responsible for the coupling to antisymmetric cladding modes.

2. TEMPERATURE DISTRIBUTION IN THE ARC DISCHARGE

The arc-induced LPFGs are created in an optical fiber through a periodical exposure along its length to arc discharges produced by a fusion splicing machine. During the writing process, the fiber is kept under longitudinal stress, which thinners and elongates the fiber section heated by the arc. Normally, the fiber is placed in the center between the electrodes. This position is the center of symmetry of the setup, and therefore it was assumed earlier that this is the optimum position, the temperature being highest and the temperature gradient being smallest here [5, 6]. However, the analysis of the symmetry of cladding modes excited by LPFGs in SMF-28 fiber has revealed that the perturbation induced in these gratings is antisymmetric. We also note that the tomographic stress profiles of the fiber region submitted to arc discharge exhibit asymmetry [7].

In order to understand the origin of the asymmetry of this perturbation, we study the temperature distribution in the arc that is applied to the fiber. In our setup, the current in the arc is direct (dc). Therefore, the arc is directional and

[*] olegivvit@yandex.ru; phone (+351) 226 082 601; fax (+351) 226 082 799

the center between the electrodes is not the center of symmetry. This can be seen in the photograph of the arc discharge in Fig. 1. The electrode at the bottom (cathode) glows only on its tip, while the electrode at the top (anode) glows in a much larger area. The arc itself is brighter near the lower electrode. Thus, we expect that there is a gradient of temperature along the line joining the electrodes as well as in the perpendicular direction along the fiber axis.

To estimate the temperature gradient in the arc, we measured the dependence of the fiber diameter reduction, in the section heated by the arc, on the position of the fiber with respect to the electrodes (in the *y*-*z* plane). The decrease in the fiber diameter is a function of fluidity of the fiber in the arc and the duration of the arc or, rather, a function of the product of the fiber fluidity and the arc duration: $\Delta D = K(tF)$. This function can be obtained by measuring the decrease in the fiber diameter for various values of arc duration or, equivalently, by applying the same discharge (having duration t_0) several times (N times) on the same fiber section ($\Delta D = K(Nt_0F_0) = G(N)$). F_0 is the fiber fluidity in the arc and is constant for all discharges. Knowing the function G, we can calculate the fiber fluidity in a different arc from the decrease in diameter upon one discharge as $F = F_0 G^{-1}(\Delta D)$, where G^{-1} is the inverse of the function G.

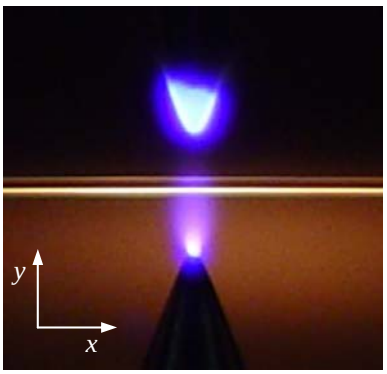

Fig. 1. Photograph of the arc discharge showing its asymmetry.

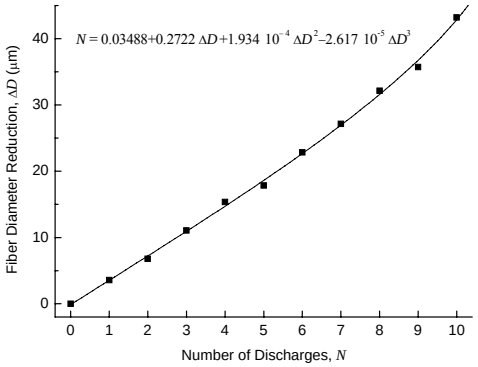

Fig. 2. Fiber diameter reduction versus number of discharges.

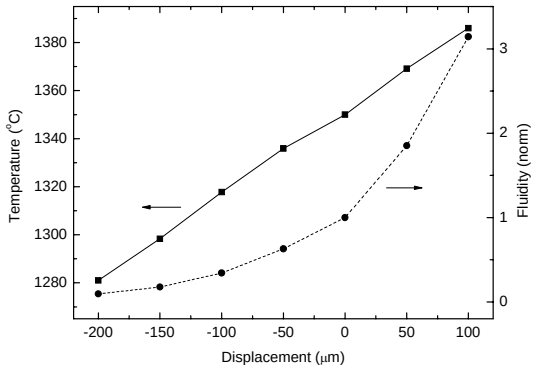

Fig. 3. Fiber temperature and fluidity along the *y* axis.

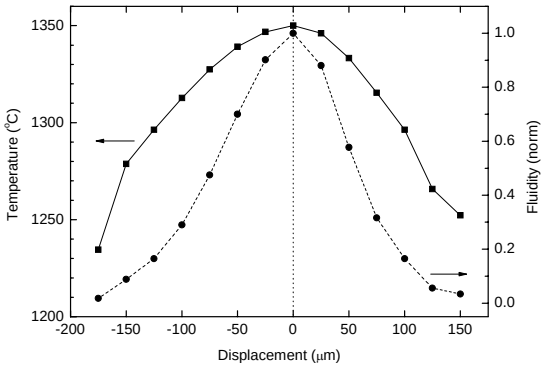

Fig. 4. Fiber temperature and fluidity along the *z* axis.

The dependence of the fiber diameter reduction on the number of discharges is shown in Fig. 2. We fitted the inverse of this dependence by a polynomial curve of the third order. The formula shown in this figure is exactly the expression for the function $G^{-1}(\Delta D)$. Then we placed the fiber in the *x*-*y* plane and measured the dependence of the fiber diameter reduction on the *y* coordinate. Using the expression for G^{-1}, we obtained the fiber fluidity, which is shown in Fig. 3. Afterwards, the temperature was calculated by using the following equation (derived from the dependence of the silica viscosity on temperature in the range 1000–1400 ºC; eq. 2 from Ref. 8):

$$\log F = 12.4 - \frac{37192}{T}, \qquad (1)$$

where F is the silica fluidity ($Pa^{-1}s^{-1}$) and T is the temperature (K). To find F_0, we assumed that the temperature of the fiber in the center between the electrodes is 1350 ºC [9]. From Figs. 3 and 4, we obtained a constant temperature gradient of ~0.35 ºC/μm along the y axis and a temperature gradient having a maximum of ~0.7 ºC/μm along the z axis.

3. ASYMMETRY OF PERTURBATION IN THE FIBER

As we have shown in the previous section, wherever in the arc the fiber is positioned, there is always a temperature gradient. The gradient is quite high: when the fiber is shifted along the y axis by the distance equal to its diameter (125 μm), the fiber fluidity changes by a factor of 2.5; the change may be even higher (with a factor of 5) when the fiber is shifted along the z axis. If the fiber is in the center between the electrodes, only the temperature gradient in the y direction is present. However, the error in the z coordinate of fiber, for example, of 20 μm creates such a temperature gradient that the fiber fluidity differs by a factor of 2 in two points separated by 125 μm. We should expect that this temperature gradient can create a strong temperature gradient inside the fiber itself. Therefore, we attempted to reveal the existence of a temperature gradient inside the fiber, which may be the asymmetric perturbation that forms the LPFG.

Two types of geometric deformation of the fiber occur in an arc discharge: tapering and microbending. The former is a symmetric diameter reduction and an elongation of the fiber. This fiber deformation induces coupling to symmetric modes. However, as we have shown recently [10] the value of the coupling constant corresponding to a typical fiber diameter reduction of a few percent is too small to explain the formation of the grating. The microbending occurs when the fiber body is locally displaced in the plane lateral to the fiber due to some asymmetry in the setup. The presence of a temperature distribution in the fiber can be this asymmetry.

We scrutinized the sections of the fiber exposed to the arc and found an asymmetry in the deformation. Fig. 5(a) shows a photograph (squeezed in the longitudinal direction) of an SMF-28 fiber with a modulation of ~5% obtained during the inscription of a 540 μm-grating where the modulation on the left side is visibly larger than on the right side. Fig. 5(b) illustrates how such a difference between the two sides of the fiber induces a core shift or geometrical microbending that may lead to the grating formation. We believe that the difference between the deformations on the opposite sides is caused by the difference in the viscosity of silica, which itself is due to the temperature difference.

To estimate the temperature difference between the two sides of the fiber heated by the arc, we placed a pressurized silica capillary into the arc instead of the fiber. The capillary was asymmetrically swollen (Fig. 6). The increase in diameter is approximately proportional to the silica fluidity. Then the difference in fluidity between the opposite sides of the capillary is a factor of 1.5-2, which corresponds to a temperature difference of about 20 °C.

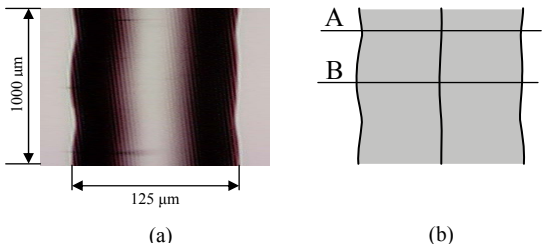

Fig. 5. (a) Photograph of a fiber with its shape modified by arc discharges; (b) shift of the fiber central line (microdeformation).

Fig. 6. Asymmetric deformation of a silica capillary (56/125 μm) submitted to an arc-discharge.

To determine the influence of the core shift on the coupling strength we use the coupled mode theory. The coupling coefficient is defined as the overlap integral between the core and cladding mode fields and the perturbation Δn induced by the core shift. The perturbation is nonzero only in the two regions one of which is near the core radius and the other is near the cladding radius. Fig. 7 (a) and (b) show the refractive index change on this fiber ($\Delta n = 0.0052$, D_{co}=8.2 μm). Δn is equal to $n_{co} - n_{cl}$ at around r_{co} and $n_{cl} - 1$ at around r_{cl}. The change at the cladding–air interface can be neglected in the calculation of the coupling coefficient because the core mode amplitude is vanishingly small at this interface. The coupling constant can be expressed as $C\pi\Delta n_{mod} I / \lambda_r$, where I is the overlap integral, λ_r is the resonance wavelength, Δn_{mod} is the refractive index modulation, and C is the constant equal to the first coefficient in the

Fourier transform of the grating pitch shape [11]. Fig. 8 shows the coupling constant as a function of the core shift for the first four cladding modes. As seen, the coupling coefficient increases with the increase in the core shift achieving 100% coupling ($kL = \pi/2$) for values in the range 0.3-0.35 μm. The value measured for the core shift from Fig. 6 is of about 0.35 μm, being, therefore, sufficient to obtain gratings with large coupling strength.

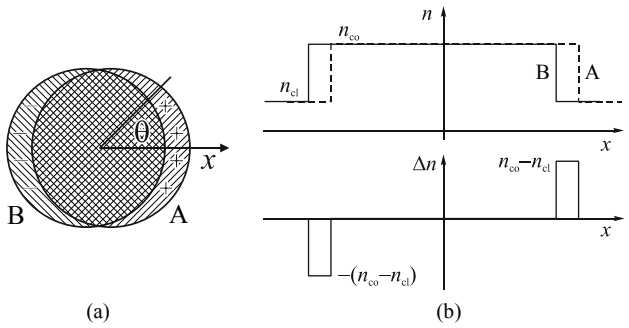

Fig. 7. (a) Refractive index change due to the shift of the fiber core; (b) refractive index change along the *x* axis.

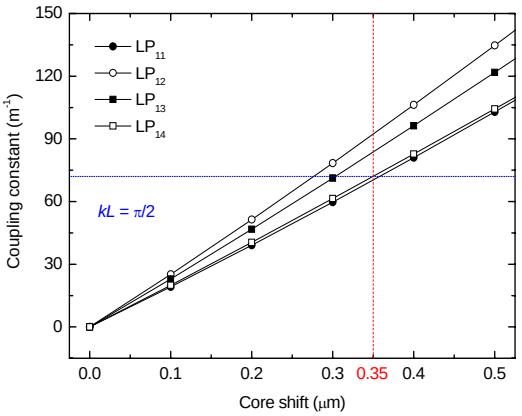

Fig. 8. Coupling constant as a function of the core shift.

4. CONCLUSION

We have demonstrated that the origin of antisymmetric perturbation of the fiber in arc-induced long-period gratings that couple the core mode into the antisymmetric LP_{1i} cladding modes is the temperature gradient in the arc discharge. We have shown that this gradient causes a temperature gradient in the fiber, which results in a gradient of viscosity and a corresponding asymmetry of fiber deformation. The effect of microdeformation consisting in periodical core shift is strong enough to produce gratings with coupling strengths measured in experiments.

REFERENCES

1. G. Rego, R. Falate, J. L. Fabris, J. L. Santos, H. M. Salgado, S. L. Semjonov, and E. M. Dianov, "Arc-induced long-period gratings in aluminosilicate glass fibers", Opt. Lett. **30**, 2065-2067 (2005)
2. G. Rego, A. Fernandez Fernandez, A. Gusarov, B. Brichard, F. Berghmans, J. L. Santos, and H. M. Salgado, "Effect of ionizing radiation on the properties of long-period fiber gratings", Appl. Opt. **44**, 6258-6263 (2005)
3. G. Rego, R. Falate, O. Ivanov, and J. L. Santos, "Simultaneous Temperature and Strain Measurements Performed by a Step-Changed Arc-Induced Long-Period Fiber Grating", Appl. Opt. **46**, (to be published)
4. G. Rego, O. Ivanov, and P.V.S. Marques, "Demonstration of coupling to symmetric and antisymmetric cladding modes in arc-induced long-period fiber gratings", Opt. Exp. **14**, 9594-9599 (2006)
5. L. Xiao, W. Jin,M. S. Demokan,H. L. Ho,Y.L. Hoo, and C. Zhao, "Fabrication of selective injection microstructured optical fibers with a conventional fusion splicer", Opt. Exp. **13**, 9014-9022 (2005)
6. M. Tachikura, "Fusion mass-splicing for optical fibers using electric discharges between two pairs of electrodes", Appl. Opt. **23**, 492-498 (1984)
7. F. Durr, G. Rego, P.V.S. Marques, S.L. Semjonov, E. Dianov, H.G. Limberger, and R.P. Salathe, "Stress Profiling of Arc-Induced Long Period Fiber Gratings", J. Lightwave Technol. **23**, 3947-3953 (2005)
8. R. H. Doremus, "Viscosity of silica", J. Appl. Phys. **92**, 7619-7629 (2002)
9. G. Rego, L. M. N. B. F. Santos, B. Schröder, P. V. S. Marques, J. L. Santos, and H. M. Salgado, "In Situ Temperature Measurement of an Optical Fiber Submitted to Electric Arc Discharges", IEEE Photon. Technol. Lett. **16**, 2111-2113 (2004)
10. G. Rego, O. Ivanov, P. V. S. Marques, and J. L. Santos, "Investigation of formation mechanisms of arc-induced long-period fiber gratings", in Proc. of OFS-18, paper TuE84 (2006)
11. S. A. Vasiliev and O. I. Medvedkov, "Long-period refractive index fiber gratings: properties, applications, and fabrication techniques," in Proc. of SPIE **4083,** 212-223 (2000)